Theoretical Investigations of Zintl Anions Analogous to Ozone

F. Hagelberg*

Department of Physics, Atmospheric Sciences and General Science, Jackson State University, Jackson, Mississippi 39217

T. P. Das

Department of Physics, State University of New York at Albany, Albany, New York 12222

K. G. Weil

Department of Materials Science and Engineering, The Pennsylvania State University, University Park, Pennsylvania 16802

Received: October 28, 1997; In Final Form: April 20, 1998

Structural features of several species based on Sb_3 as a nuclear unit are investigated by ab initio analysis. In particular, the applicability of the Zintl−Klemm−Busmann (ZKB) principle on alkali−antimony clusters of the form A_3Sb_3 and $A_4Sb_3^+$ (A = Na, K, Rb) is examined, which have been detected by mass spectrometric measurements. It is shown that basic properties pertaining to geometry, bonding, and stability of these 18 valence electron units display a clear analogy to the respective features of the isoelectronic ozone molecule. We conclude that A_3Sb_3 represents a case in which the ZKB principle, so far almost exclusively applied to solids and liquids, is valid for the gaseous phase as well. An extension of the ZKB principle, which according to its traditional meaning involves transfer of charge, to spin-transfer processes is proposed. Possible experimental tests regarding the geometries of the species investigated are pointed out.

I. Introduction

The Zintl concept has been used very successfully in the explanation of structures and bonding features of numerous condensed matter systems.[1,2] In its generalized form due to Schaefer, Eisenmann, and Mueller[3] it states the structural invariance of an element with valence electron number N under replacement of some of its atoms by an element with valence electron number $N - M$, provided the missing M electrons are supplied through the addition of M alkali metal atoms that function as electron donors. This is the content of the "ZKB principle". Wherever this principle holds, the structure of a compound will be determined by its valence electron count rather than by the elemental identities of its constituents.

In recent theoretical investigations, the applicability and validity of the ZKB principle to antimony-based atomic clusters has been explored.[4] These previous studies have focused on molecular systems based on the extraordinarily stable Sb_4 unit.[5] This system displays the ground-state structure of a regular tetrahedron,[6,7] which is plausible in view of the tendency of each Sb constituent of Sb_4 to approach an octet configuration in the valence shell as closely as possible. The stability of the tetrahedral geometry of the Sb_4 cluster under isoelectronic substitution of an A−Sn unit (A = alkali metal atom) for one Sb atom has been demonstrated by ab initio calculations.[4] Electron transfer from the alkali metal species leads to the formation of the anion $(Sb_3Sn)^-$ whose structural and bonding characteristics exhibit only very slight deviations from Sb_4.

The Sb_4 unit, however, is very sensitive to changes of its valence electron count of 20. In a series of ab initio investigations, Sb_4-based systems with 22, 24, and 26 valence electrons, namely, A_2Sb_4, A_4Sb_4, and A_6Sb_4, have been explored.[8] In these complexes, the T_d symmetry of the free Sb_4 cluster is found to flatten out into D_{4h} symmetry. This structural transition can be shown to proceed as a consequence of Jahn−Teller distortion associated with the transfer of additional electrons to a 20-valence-electron tetramer of T_d symmetry. Preferentially, the Sb_4 cluster as a part of an $A_{2N}Sb_4$ (N = 1, 2, 3) unit exists as a square-shaped Sb_4^{2-} anion. The D_{4h} symmetry of the 2-fold ionic species, in turn, is Jahn−Teller forbidden for the neutral Sb_4 unit. Thus, the electron transfer that occurs from the alkali cage to the antimony cluster nucleus can be interpreted to remove the ground-state degeneracy for a 20-valence-electron tetramer in D_{4h} symmetry. All alkali−antimony units analyzed so far contain a Sb_4 cluster nucleus that closely resembles the free Sb_4^{2-} unit, in view of both its square geometry and its electronic structure.

Numerous species representing Sb_4-based Zintl clusters and alkali−antimony clusters have been isolated by Knudsen effusion mass spectrometry.[9] Using the gas aggregation technique, Hartmann and Castleman[10] were able to generate a large series of sodium−antimony clusters of the form Na_xSb_y where x varies between 1 and 12, y between 2 and 16. Besides Sb_2- and Sb_4-based species, a number of Na_xSb_3 systems have been detected in the sodium−antimony vapor.

In the present work, we aim at an understanding of both structural and bonding features of a different class of Sb-based clusters rather than the Sb_4-containing systems theoretically studied so far,[4,8] namely, Zintl anions based on Sb_3, with particular emphasis on the analysis of A_3Sb_3 units. Species of the form A_2Sb_2 can be understood as O_2-analogous Zintl systems.[11] It will be shown here by arguments relying on first principles calculations that bonding mechanisms and possible

S1089-5639(98)00004-8 CCC: $15.00
Published on Web 05/23/1998

geometries of A_3Sb_3 are closely related to those found in the O_3 molecule. Comparing units with different alkali constituents (A = Na, K, Rb), we will show that the similarity between A_3Sb_3 and ozone becomes more pronounced with increasing electron transfer from the alkali to the antimony atoms. In accordance with the Zintl concept, we will thus interpret the valence electron structure of A_3Sb_3 as a realization of a prototypical scheme defined by ozone. A number of additional equilibrium geometries result from our analysis. All possible structures identified for the cluster A_3Sb_3 will be demonstrated to be stabilized through electron transfer from the alkali to the antimony subsystem by which a Jahn−Teller degeneracy is lifted. This feature constitutes a clear parallel of the present investigations to our previous ones on alkali−antimony systems containing the Sb_4 unit.[8] A similar line of arguments will lead to an ozone analogy of the unit ASb_3 in a spin triplet configuration, with spin transfer instead of charge transfer taking the role of the stabilizing process.

II. Procedure

In this work, we have carried out theoretical investigations on three Sb_3-based cluster systems, namely, A_3Sb_3, A_4Sb_3, and ASb_3 (A = Na, K, Rb). The guiding point of interest is their structural similarity to the ozone molecule. Although it is a well-established result that ozone exhibits two stable geometries, that is, a C_{2v} ground state with an opening angle of $\alpha = 116.49°$ and a D_{3h} isomer,[12,13] no investigations with respect to geometric and bonding features have been performed so far on the Sb_3-based systems indicated above.

For each individual molecular system considered, we obtained equilibrium geometries through total energy minimization using the Hartree−Fock procedure. The total cluster energy was varied as a function of all interatomic distances and bond angles until an energy minimum was found corresponding to either the ground state or a stable isomer of the respective species. To economize on the computational effort, we used effective core potentials[14−16] in all cases discussed in section III. The pseudopotentials employed incorporate one-electron relativistic effects, which are of relevance in view of the high atomic numbers of most cluster constituents considered in this work.

In all calculations presented here, double-ζ basis sets[14−16] were used in conjunction with polarization functions of d angular symmetry.[17] In the geometry optimization carried out for alkali−antimony systems, the electron correlation effect was treated in the framework of Moller−Plesset perturbation theory in second order ("MP2").

We subjected the adequacy of this theoretical approach to a number of tests. Since the goal of this work is a description of structural features of Sb_3-based clusters, a correct representation of the nuclear Sb_3 unit is of crucial importance for the research reported here. We compare the results of our work with those of Balasubramanian et al.[18] who investigated the Sb_3 unit by a considerably more complex procedure than the one used here, involving a complete active space multiconfiguration method followed by multireference configuration interaction (CASMC-SCF-MRCI) to account for many-body effects.

As will be outlined further in section III, we identified for the Sb_3 unit a ground state of $^2A_2$ symmetry, exhibiting the geometry of a slightly compressed isosceles triangle. Although this finding is in keeping with the results communicated in ref 18, we obtain for the two Sb−Sb bond lengths present in Sb_3 values $D_{1,2}$ that somewhat differ from those emerging from the CASMCSCF-MRCI procedure. However, comparing the respective results (D_1 = 2.74 Å, D_2 = 2.95 Å from the MP2 treatment; D_1 = 2.76 Å, D_2 = 2.99 Å from the CASMCSCF-MRCI treatment), one realizes that the differences between both procedures are about 1%. Thus, both computational techniques arrive at well-converging predictions pertaining to the Sb_3 geometry. A similar observation was made in ref 4 where the tetrahedral Sb_4 unit was investigated using the MP2 method described above. It was found that the MP2 result for the Sb−Sb bond length deviates from the corresponding CASMCSCF-MRCI result by less than one per mil.

Two experimental quantities not directly related to the molecular geometry provide secondary tests for the validity of the approach used in this work: the ionization potential of Sb_3 [19] and the atomization energy of Sb_3.[20] Cabaud et al. give a value of 7.5 ± 0.13 eV for the ionization potential. Calculating the total energy of Sb_3^+ at the ground-state geometry of Sb_3, we obtain the value 6.52 eV. Although this is somewhat lower than the experimental finding, it agrees with the result of a more complex computation at the CASSCF level.[18] Since it has been shown that an MRCI treatment improves significantly upon the theoretical value for the Sb_3 ionization potential, yielding 7.1 eV, one can expect that further refinement in the description of the electron correlation effect in combination with an extension of the Gaussian basis set used will close the remaining gap between theory and experiment.

A similar underestimation of the measured result compared with the calculated one was found when evaluating the atomization energy of Sb_3. This quantity was obtained using the same computational procedure in the calculation of total energies for both the molecule and its atomic constituents at infinite distance from each other. Whereas Gingerich et al. report a value for this quantity of 1.86 ± 0.002 eV/atom,[20] our calculation yields 1.04 eV/atom. Again, it will be worthwhile investigating to what extent this difference is due to not quite sufficient incorporation of many-body effects into the presently used approach.

All atomic charges given in section III have been evaluated using Mulliken population analysis[22] based on the Moller−Plesset perturbation treatment outlined above.

It must be noted that various quantum chemical facets of the ozone ground state, and thus probably also of the ground states of ozone analogous systems, require for adequate description computational procedures of higher complexity than those used in this work.[13] Since, however, the emphasis of this research is on qualitative tendencies rather than on accurate quantitative results and since the consistent use of more appropriate many-body perturbation theory models[13] for all systems discussed here would be a prohibitively time-consuming task, the presently adopted approach appears justifiable.

The computational work presented here has been performed partly on the IBM RISC 6000 computer cluster system of the Cornell national supercomputer facility, partly on a private DEC 5000/133 workstation. The program GAUSSIAN 92[21] has been used for all Hartree−Fock and post-Hartree−Fock investigations of the systems that form the topic of this article.

III. Results and Discussion

We will comment first on our investigations of both the free Sb_3 unit and the Zintl anion Sb_3^{3-}. The observations made on these systems will serve as reference points for the understanding of the alkali−antimony complexes A_3Sb_3 and ASb_3, which will be discussed in the subsections b and c of this section.

(a) Units Sb_3 and Sb_3^{3-}. For both trimers, complete ab initio geometry optimizations have been carried out as a function of the Sb_3 opening angle (see Figure 1). The potential curve for

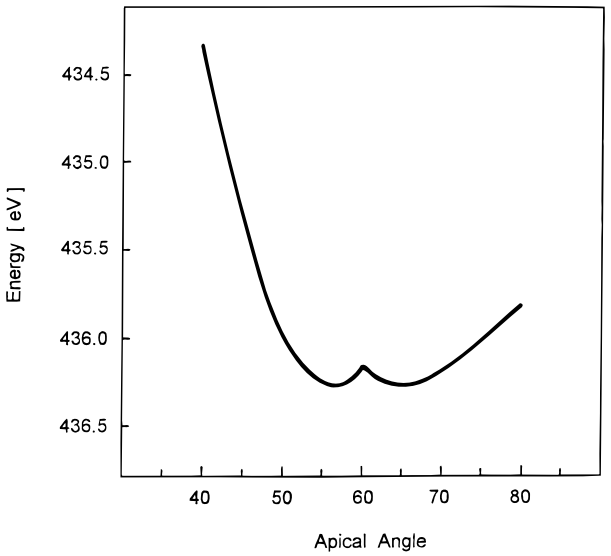

Figure 1. Minimum cluster energy vs apical angle for Sb_3 around the point of equilateral geometry ($\alpha = 60.0°$). For each angle, all interatomic distances were optimized.

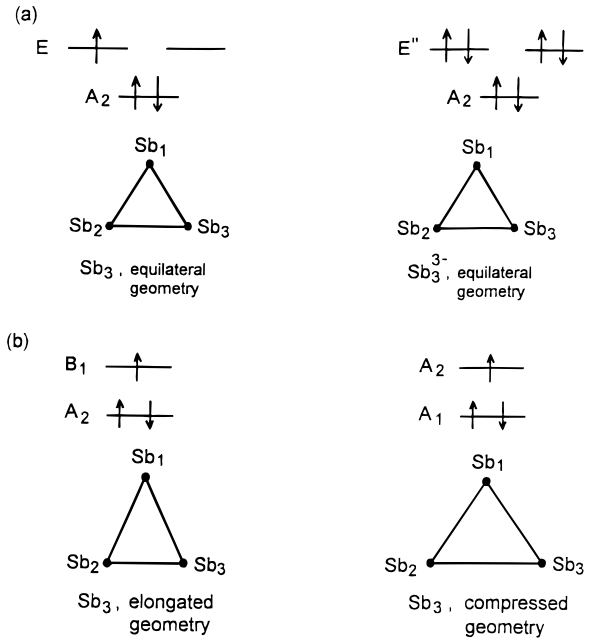

Figure 2. Term schemes of highest occupied states and geometries for Sb_3 and Sb_3^{3-}: (a) Sb_3 and Sb_3^{3-} in equilateral geometry; (b) two stable geometries of Sb_3 around $\alpha = 60.0°$ resulting from distortion of the equilateral structure.

the neutral species exhibits three local minima corresponding to three equilibrium geometries; Sb_3 can be stable as a linear molecule and also as an elongated or compressed isosceles triangle where the angles of minimal energies, as found from our calculation, amount to $\alpha = 56.69°$ for the elongated variant and $\alpha = 65.25°$ for the compressed variant of the molecule. Figure 1 shows these two minima. In the given representation, the total energy of Sb_3 is plotted versus the apical angle α. For each angle chosen, the energy was minimized as a function of all interatomic distances.

The two equilibrium geometries around $\alpha = 60°$ are plausible in view of the Jahn−Teller instability of Sb_3 in D_{3h} symmetry. The HOMO of an equilateral triangle of three Sb atoms has E symmetry and is occupied by one electron only (see Figure 2a). Therefore, the ground state of Sb_3 in D_{3h} symmetry is degenerate. The HOMO can have the symmetry of either component of the D_{3h} E doublet. Following the nomenclature used in ref 23, we label these two components $E_1 = 2\Phi_1 - \Phi_2 - \Phi_3$ and $E_2 = \Phi_2 - \Phi_3$ where the indices 1, 2, and 3 refer to the number of the respective Sb constituents in Figure 2. If the system occupies E_1, a bonding situation between atoms 2 and 3 will arise, and the resulting structure will be an elongated triangle, while a HOMO of E_2 type is antibonding with respect to atoms 2 and 3 and therefore leads to the formation of a compressed triangle. From our calculations, the geometry of this compressed triangle seems to be preferred over the other two equilibrium geometries of the Sb_3 system, being deeper in total energy than the elongated triangle by an amount of $\Delta E = 0.02$ [eV] and deeper than the linear variant by $\Delta E = 2.03$ [eV].

From the the highest occupied levels in Sb_3 (see Figure 2a), it is obvious that the metastable 3-fold anionic species of the molecule can adopt the geometry of an equilateral triangle. Addition of three electrons will completely fill the E level, which is partially occupied in the neutral system, and therefore removes the pseudo-Jahn−Teller instability.[24] At the same time, in the linear variant of the molecule, an incompletely filled degenerate HOMO state is produced that couples with a bending mode and leads to Renner−Teller distortion.[25] Both these qualitative predictions are confirmed by the calculated Sb_3^{3-} potential curve as displayed in Figure 3a, which was calculated on the level of Hartree−Fock theory. This curve is characterized by two clearly pronounced minima, one corresponding to the equilateral variant of Sb_3^{3-} and the second one to an isosceles variant with a large opening angle of $\alpha = 130.7°$. For the latter geometry, our calculation yields a minimum energy slightly lower than the one found for the equilateral structure by an amount of $\Delta E = 0.5$ [eV]. We propose therefore the isosceles variant with a large opening angle as the most stable geometry of the Sb_3^{3-} anion. Both minima are separated by a saddle point at $\alpha = 76.9°$.

Strictly analogous observations are made in a first principles study of the ozone molecule, carried out on the basis of the Hartree−Fock procedure, as shown in Figure 3b. Again, the potential curve defines two minima, one at $\alpha = 60°$, the other one at a markedly larger angle, $\alpha = 119.6°$, which is close to the experimental finding of $\alpha = 116.5°$ [12] and corresponds to the absolute energy minimum of the molecule. However, it must be pointed out that parts a and b of Figure 3 are included only for qualitative illustration of the structural analogy between O_3 and Sb_3^{3-}. As is well-known (see, for instance, ref 13), the Hartree−Fock procedure is inadequate for a quantitative analysis of the bonding situation in ozone.

The structural characteristics of the dianion Sb_3^{2-} closely resemble not only those of the neutral Sb trimer but also those of the trianion Sb_3^{3-}. While subjected to Jahn−Teller distortion at equilateral geometry, Sb_3^{2-} does not distort as strongly as Sb_3. According to our calculations, Sb_3^{2-} stabilizes as an elongated or compressed isosceles triangle with apical angles 56.7° or 63.2°, both values being closer to 60° than the respective angles obtained for Sb_3. This finding will be of interest in the interpretation of the species A_3Sb_3.

(b) Systems A_3Sb_3 and $A_4Sb_3^+$. The findings reported under section a about the adiabatic potential curve of Sb_3^{3-} might hold the key for the understanding of the A_3Sb_3 systems that are the focus of the present work. Owing to the marked electronegativity difference between Sb and all alkali species,[26] in all units of the form A_3Sb_3, sizable electron transfer will occur from the alkali to the antimony subsystem. Therefore, the possible geometries and bonding characteristics of Sb_3 as part of the A_3Sb_3 cluster will be between the those of the free Sb_3 molecule

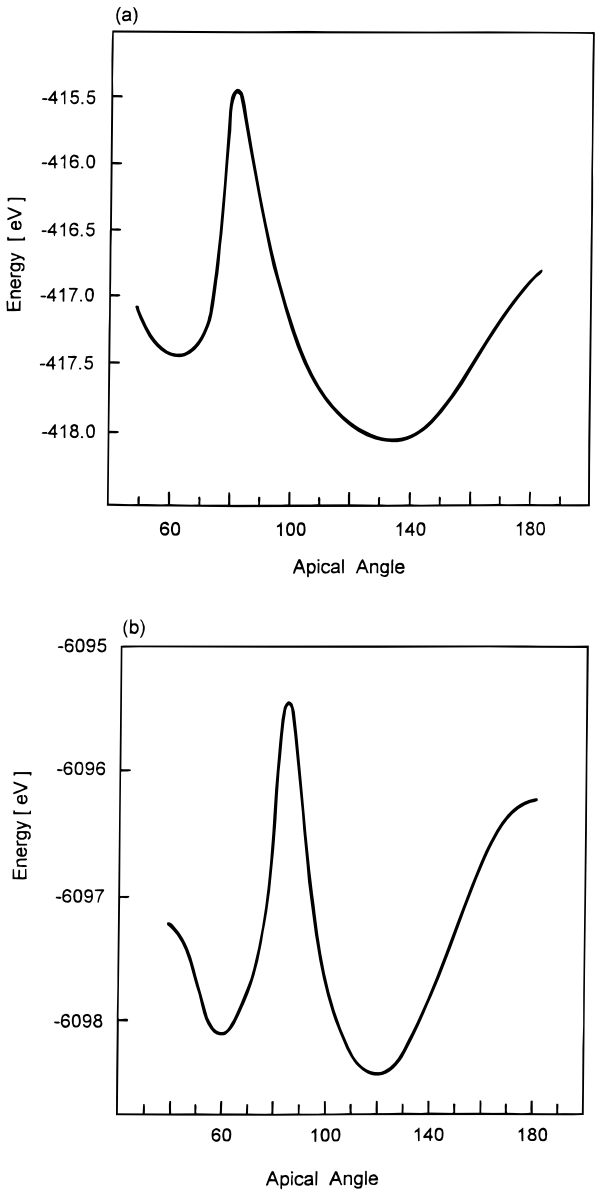

Figure 3. Potential curves for (a) Sb_3^{3-} and (b) O_3.

and those of the Sb_3^{3-} anion. Guided by the observations made on the potential curves of Sb_3 and Sb_3^{3-}, one could expect the experimentally detected Na_3Sb_3 cluster to exist in at least two possible equilibrium variants, the first containing the Sb_3 unit as an isosceles triangle with a large opening angle, the second with an Sb_3 subsystem of close to equilateral structure. Carrying out geometry optimizations, we isolated three energy minima. Besides an isosceles variant with an opening angle of 109.8°, our calculations yield two other isosceles variants with opening angles close to those found for the possible geometries of the free Sb_3 unit: $\alpha = 57.48°$ and $\alpha = 64.13°$. In contrast to the free Sb_3 system, however, the larger of the two angles now corresponds to the absolute energy minimum of the molecule (compare Table 1). In the energetically preferred structure, the highest two occupied levels arise from the E doublet of the D_{3h} group, exhibiting the characteristic $\Phi_2 - \Phi_3$ and $2\Phi_1 - \Phi_2 - \Phi_3$ symmetries in the MO coefficients of the three Sb constituents. Since the present structure deviates from D_{3h} geometry, however, the two levels are separated by a small energy difference, the $\Phi_2 - \Phi_3$ state lying 0.08 eV below the $2\Phi_1 - \Phi_2 - \Phi_3$ state. Although electron transfer, proceeding from the alkali to the antimony cluster constituents, thus leads

TABLE 1: Minimal Energies and Sb_3 Opening Angles from MP2 Geometry Optimization for the Isomers of Sb_3 and A_3Sb_3 (A = Na, K, Rb) Identified in This Work[a]

system	opening angle [deg]	energy [eV]	charge on A_3
	A. Strongly Compressed Variant		
Na_3Sb_3	111.39	−454.44	1.32
K_3Sb_3	116.64	−451.46	1.82
Rb_3Sb_3	118.60	−450.41	1.84
	B. Compressed Variant		
Sb_3	65.30	−436.28	
Na_3Sb_3	64.135	−454.61	1.47
K_3Sb_3	63.60	−451.55	2.03
Rb_3Sb_3	63.58	−450.38	2.03
	C. Elongated Variant		
Sb_3	56.69	−436.26	
Na_3Sb_3	57.70	−454.56	1.43
K_3Sb_3	57.96	−451.39	1.93
Rb_3Sb_3	57.97	−450.27	1.92

[a] For the A_3Sb_3 species, the charges on the alkali subsystem are also given.

to the population of both states, the molecular orbital that is antibonding in the atoms 2 and 3 influences the geometry of the Sb_3 unit more than the bonding orbital that results in an opening angle $\alpha > 60.0°$. In the elongated variant of the Na_3Sb_3 molecule, we find this situation reversed. Here, the $2\Phi_1 - \Phi_2 - \Phi_3$ level lies deeper by an energy $\Delta E = 0.13$ eV than the $\Phi_2 - \Phi_3$ level.

The trend toward both reduction of the energy gap between the two HOMOs and realization of equilateral Sb_3 symmetry is reflected by the electron transfer between alkali and antimony subsystems. According to a Mulliken population analysis,[22] the sum of the positive charges on all three sodium atoms is slightly higher in case of the preferred structure, compared with the alternative structure, involving an elongated Sb_3 triangle.

Whereas our calculations yield only a small energy difference of $\Delta E = 0.05$ eV between the two geometric variants that contain Sb_3 in a near-equilateral form, the third energy minimum identified is higher than the two discussed above, being separated from the absolute minimum by a difference of $\Delta E = 0.17$ eV. This feature introduces a marked distinction between the systems Na_3Sb_3 and Sb_3^{3-}, the latter unit being characterized by an absolute energy minimum at a large opening angle of $\alpha = 130.7°$ and a local minimum at $\alpha = 60.0°$. Summarizing our results of the Sb_3 cluster nucleus of Na_3Sb_3, we might say that it behaves like a hybrid between the neutral Sb_3 and the anionic Sb_3^{3-} molecule. Although the existence of two minima around equilateral geometry likens the Sb_3 cluster nucleus to the free Sb_3 species, the emergence of a third equilibrium at a large opening angle draws a parallel to Sb_3^{3-} and thus to O_3. The observation, however, that the Sb_3 analogous minima seem to be energetically favored over the Sb_3^{3-} analogous one makes the Na_3Sb_3 cluster nucleus appear somewhat more similar to Sb_3 than to Sb_3^{3-}.

The features outlined above could change as the charge transfer from the alkali to the antimony subsystem changes. It is thus interesting to repeat the calculations discussed, replacing A = Na by the larger alkali atoms K and Rb in A_3Sb_3. Other alkali atoms could be included in these considerations; however, we restricted our calculations to the three alkali species Na, K, and Rb, which in principle can be produced in the laboratory without major difficulty. Considering the enhanced electronegativity difference between Sb and K or Rb compared with those of Sb and Na, one will expect the properties of the Sb_3 cluster nucleus of A_3Sb_3 to shift toward those of the Sb_3^{3-} anion and away from those of the neutral Sb_3 unit as one goes from A =

TABLE 2: Symmetrized Forces for Systems of the Form A_3Sb_3 (A = Na, K, Rb)[a]

system	reduced force matrix element $[e^2/a_0^2]$
(a) Forces Tending toward Elongation	
Na_3Sb_3	0.012
K_3Sb_3	0.011
Rb_3Sb_3	0.010
(b) Forces Tending toward Compression	
Na_3Sb_3	0.015
K_3Sb_3	0.014
Rb_3Sb_3	0.013

[a] The Sb_3 subsystem is stabilized in D_{3h} symmetry.

Na to A = K, Rb. We confirmed this by performing geometry optimizations for K_3Sb_3 and Rb_3Sb_3. In both cases we could identify the three equilibrium structures described in the context of our discussion of Na_3Sb_3. A general feature that distinguishes the systems A_3Sb_3 with A = K, Rb from Na_3Sb_3 is a marked enhancement of charge transfer from the alkakli to the antimony subsystem in all three equilibrium geometries (see Table 1) for both A = K and A = Rb. Mulliken population analysis yields an average increase of positive charge on the three alkali metal atom constituents in K_3Sb_3 and Rb_3Sb_3 over the ones in Na_3Sb_3 of approximately 30%. This enhancement of charge transfer is correlated to a number of crucial differences between the species under examination. We will comment first on the two Sb_3 analogous minima close to equilateral geometry.

As is obvious from Table 1, the opening angles α of the isosceles Sb_3 triangles in K_3Sb_3 and Rb_3Sb_3 are closer to the limit of $\alpha = 60.0°$ than in case of Na_3Sb_3. This behavior reflects the trend observed in our study of the pure anionic systems Sb_3^{3-} and Sb_3^{2-} (see above), where a sensitive change of the opening angle toward $\alpha = 60.0°$ was found with the increase of negative charge attached to the Sb_3 unit from 1 to 2 elementary charges. Since this increase is smaller in the present case, amounting only to approximately 0.5 elementary charges (see Table 2), the associated geometric change is less pronounced although clearly noticeable.

Since the two stable geometries identified close to the equilateral structure result from Jahn−Teller distortion of that structure, the difference between the shapes of the Sb_3 cluster nucleus in Na_3Sb_3 and K_3Sb_3 (Rb_3Sb_3) must be rooted in different deformation forces acting on an equilateral Sb_3 unit in the various A_3Sb_3 species compared with each other. As a test for the validity of this conclusion, we carried out optimizations of A_3Sb_3 (A = Na, K, Rb) in which the Sb_3 subsystem was constrained to maintain equilateral geometry. For each species investigated, two possible structures result from these calculations corresponding to the two components of the E″ doublet in D_{3h} symmetry. In the first case, charge transfer proceeds from the alkali metal atoms to predominantly one of the Sb atoms. If this possibility is realized, the $2\Phi_1 - \Phi_2 - \Phi_3$ level is more strongly populated than the $\Phi_2 - \Phi_3$ level, and the distorting force will tend toward elongation of the Sb_3 triangle. In the second case, the two E″ levels exchange their roles; i.e., the alkali metal atoms arrange themselves such that the larger part of the transferred charge is placed symmetrically on two of the Sb atoms. This situation gives rise to a force that leads to the compression of the Sb_3 triangle. For each of the six resulting cases, we calculated symmetrized forces according to the scheme displayed in Figure 4. Table 2 summarizes the reduced force matrix elements that we derived from the two components F_x and F_y. As can be seen from these values, slightly larger distortion forces are found in Na_3Sb_3 than in K_3Sb_3 (Rb_3Sb_3), in accordance with our observation that the geometry of the Sb_3 unit is somewhat closer to the equilateral structure in the two latter systems than in the former. It should be noted that the forces that tend toward compression of the Sb_3 triangle are consistently larger than those that tend toward elongation. This finding agrees with the above statement that the equilibrium energies of the elongated A_3Sb_3 variants are, from our calculation, throughout higher than those of the compressed A_3Sb_3 variants.

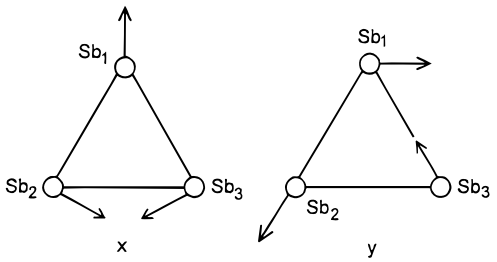

Figure 4. Symmetrized coordinates *X* and *Y* used in the definition of generalized forces (see text).

In the following, we want to comment on the third geometric variant identified for A_3Sb_3. This variant is characterized by a strongly compressed Sb_3 triangle with apical angles α in the range between 110° and 120° (see Table 1) geometry, in analogy to the ground-state structures of O_3 and Sb_3^{3-} as described in section III(a). For Na_3Sb_3, we find this strongly compressed variant clearly higher in energy than the compressed variant, both mimimum energies being separated by $\Delta E = 0.17$ eV. However, as one goes from from A = Na to A = K, Rb and thus in a direction of increasing electron transfer to the Sb_3 unit, one finds a diminished energy gap between the two geometric alternatives of $\Delta E = 0.09$ eV for A = K and a slight preference of the strongly compressed over the compressed variant for A = Rb. These differences correspond to a substantially higher charge transfer from the alkali to the antimony subsystem for A = K in comparison to A = Na and a somewhat higher charge transfer for A = Rb in comparison to A = K (see Table 1). As already observed in the context of the minima around $\alpha = 60.0°$, the amount of electron transfer appears to be a crucial parameter for the definition of the cluster geometry. With increasing negative charge on the Sb_3 cluster nucleus, the opening angle of the strongly compressed variant widens and thus moves more closely to the value $\alpha = 130.7°$ characteristic for the pure Sb_3^{3-} anion (see section III(a)).

From our considerations, the 18-valence-electron system A_3Sb_3 has turned out to be strongly determined, with respect to both structural and bonding features, by the electron transfer from the alkali subsystem to the Sb_3 cluster nucleus. The demonstrated similarity of A_3Sb_3 to the 18-electron systems O_3 and Sb_3^{3-}, which is discussed in section III(a), leads to the conclusion that the alkali metal components of the complexes examined mainly act as electron donors whose function is to bring the Sb_3 cluster nucleus as close as possible to a stable electron count of 18. If this interpretation of measured and calculated data is correct, an A^+ core added to the system A_3Sb_3 should not have any strong impact on its geometry, since it does not contribute any additional valence electrons. Experimentally, the $Na_4Sb_3^+$ ion has been detected.[10] This species can be understood as a combination of Na_3Sb_3 and a single Na^+ cation. In light of the Zintl concept, one expects thus the equilibrium geometries of the cluster nucleus of $Na_4Sb_3^+$ to exhibit the same features as found for Na_3Sb_3. Our geometry optimization for the $Na_4Sb_3^+$ species indeed yields the three minima characteristic for A_3Sb_3 (see Table 3). For the two

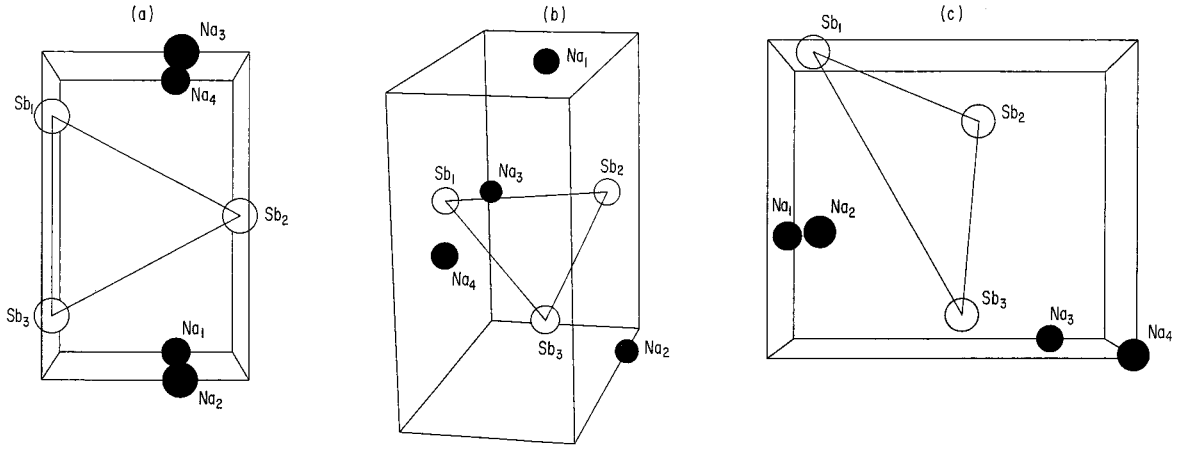

Figure 5. Three stable structures isolated for $Na_4Sb_3^+$: (a) geometry of $Na_4Sb_3^+$ containing Sb_3 as an elongated triangle; (b) geometry of $Na_4Sb_3^+$ containing Sb_3 as a compressed triangle; (c) geometry of $Na_4Sb_3^+$ containing Sb_3 as a strongly compressed triangle.

TABLE 3: Minimal Energies, Sb_3 Opening Angles, and Charges on the Alkali Subsystem from MP2 Geometry Optimization for the Isomers of $Na_4Sb_3^+$ Identified in This Work[a]

system	opening angle [deg]	energy [eV]	charge on A_4
I	56.14	−448.42	2.42
II	62.28	−448.47	2.48
III	106.44	−448.06	2.22

[a] System I contains Sb_3 as an elongated triangle, system II as a compressed triangle, and system III as a strongly compressed triangle (see text for further description of the three geometric variants).

equilibrium structures around $\alpha = 60.0°$, we find the two highly symmetric arrangements of the four Na atoms displayed in parts a and b of Figure 5, each surrounding an isosceles cluster nucleus.

The similarity between the strongly compressed variants of Na_3Sb_3 and $Na_4Sb_3^+$ is obvious. The apical angle of the cationic species, $\alpha(Na_4Sb_3^+) = 106.4°$ is somewhat reduced compared with the neutral one, $\alpha(Na_3Sb_3) = 111.4°$. This relation, as well as the feature that the deviation from isosceles structure is slightly larger for $Na_4Sb_3^+$ than for Na_3Sb_3, can be correlated with the geometry displayed in Figure 5c. Two of the four Na atoms are located much more closely to the tip atom Sb(3) than to the tip atom Sb(1). Therefore, the electron transfer proceeds preferentially to Sb(3), resulting in a sizable difference in the charges on the two tip atoms.

(c) The Systems ASb_3. Molecules of the form ASb_3 have been experimentally detected by Knudsen mass spectrometry[9] as well as by use of the gas aggregation technique.[10] They are expected to behave analogously to the singly charged anion Sb_3^-. Whatever component of the E doublet constitutes the HOMO of the Sb_3 subsystem would be completely filled through electron transfer, giving rise to stretching or compression effects. These predictions, however, are based on the assumption of a spin singlet state ($S = 0$). If a spin triplet situation is investigated, the Sb_3 unit will be stabilized by a different mechanism. With reference to the term scheme of the highest occupied Sb_3 levels (see Figure 2a), one might assume that the donor electron will be promoted into the LUMO level of the Sb_3 unit, the alkali metal atom acting as a spin donor in this case. Owing to the constraint $S = 1$, both E components will then be half-filled. Depending on the efficiency of this transfer process, an equilateral Sb_3 molecule can therefore result as the equilibrium structure in the spin triplet case.

We have examined this possibility for ASb_3 molecules with A = Na, K, Rb and found the geometry of an equilateral triangle

TABLE 4: Data Related to the System ASb_3

system	$R(Sb_1-Sb_2)$ [Å]	$R(Sb_2-Sb_3)$ [Å]	$R(Sb_3-Sb_1)$ [Å]	energy [eV]
(a) Geometries and Equilibrium Energies of the Systems ASb_3 (A = Na, K, Rb) in Spin Triplet Configuration for the C_{3v} Minimum[a]				
$NaSb_3$	3.002	3.002	3.002	−437.13
KSb_3	2.985	2.985	2.987	−436.21
$RbSb_3$	2.983	2.983	2.985	−435.96
(b) Geometries and Equilibrium Energies of the Systems ASb_3 (A = Na, K, Rb) in Spin Singlet Configuration[a]				
$NaSb_3$				
elongated	3.098	3.098	2.806	−436.83
compressed	2.818	2.818	3.455	−436.83
KSb_3				
elongated	3.114	3.114	2.804	−435.74
compressed	2.807	2.807	3.425	−435.74
$RbSb_3$				
elongated	3.111	3.111	2.806	−435.47
compressed	2.807	2.807	3.431	−435.47

(c) Comparison of the Two Stable Variants of ASb_3 in Spin Triplet Configuration

system	symmetry	opening angle [deg]	energy [eV]
$NaSb_3$	C_{3v}	60	−437.13
	C_{2v}	106.94	−440.10
KSb_3	C_{3v}	60	−436.21
	C_{2v}	107.93	−439.01
$RbSb_3$	C_{3v}	60	−435.96
	C_{2v}	109.12	−438.74

[a] $R(Sb_i-Sb_j)$ = distance between Sb atom i and Sb atom j.

for Sb_3 realized in all three systems, the alkali metal species being located on an axis through the midpoint of the Sb_3 triangle and perpendicular to its plane. For KSb_3, a very slight asymmetry in the placement of the alkaki metal atom induces small differences between the Sb−Sb bond lengths of the order of 7×10^{-4} (see Table 4a.); in the remaining two cases, the bond length differences amount to less than 10^{-5}. However, none of these deviations from D_{3h} symmetry are significant, considering the limitations in the accuracy of the computation method utilized.

In accordance with this geometric finding, an inspection of the molecular orbitals yields that the two highest occupied levels of the ASb_3 system are perfectly degenerate. This result indicates an analogy between $NaSb_3$ in triplet spin configuration and the pure Sb_3^{3-} ion. Whereas in the latter case the D_{3h} symmetry and degeneracy of the HOMO level is achieved by electron transfer, in the former case these features are established

through spin transfer. It should be noted that in complexes of the form A_3Sb_3, the equilateral shape of the Sb_3 unit is only approximated while in the spin triplet configuration of ASb_3, this form seems to be fully realized.

Inspection of the system ASb_3 in spin singlet configuration yields the two expected minima at elongated and compressed Sb_3 geometry. As is obvious from parts a and b of Table 4, both of these equilibrium structures are found to be higher in energy than either of the two geometries, resulting in a spin triplet configuration for ASb_3. Thus, ozone-analogous conditions seem to be favored in the system ASb_3.

The systems discussed in the present context give an example of a situation in which the Zintl concept, traditionally referring to structural invariance associated with the compensating action of charge donors, can be extended to spin donors as well.

To establish the full analogy of ASb_3 ($S = 1$) to A_3Sb_3 and therefore to ozone, one has to show that there also exists a stable variant of the ASb_3 ($S = 1$) species in C_{2v} symmetry with a large Sb_3 opening angle, since this latter geometric variant has turned out to be the ground state of A_3Sb_3 in cases of sufficiently high electron transfer (compare section III(b)). Indeed, this geometry has been found for each of the three systems investigated (see Table 4b). One notes that the Sb_3 opening angle increases from A = Na to A = Rb, as was already observed in the strongly compressed variant of A_3Sb_3. In case of the ASb_3 ($S = 1$) molecule, however, the C_{2v} state turns out to be consistently lower in energy than the C_{3v} state, whereas A_3Sb_3 gradually approximates the large angle ozone ground state as the electron transfer from A_3 to Sb_3 increases in strength. This feature implies a closer similarity of ozone to ASb_3 ($S = 1$) than to A_3Sb_3.

IV. Conclusion

Alkali−antimony systems based on the Sb_3 unit have been investigated in this work using ab initio computational procedures. We established a structural analogy between the 3-fold negative Sb_3^{3-} species and the ozone molecule, both representing trimers with 18 valence electrons. Both units stabilize in C_{2v} symmetry, their ground-state geometries being characterized by large opening angles. The Jahn−Teller instability, which occurs for 15-valence-electron trimers in D_{3h} symmetry, is removed as three more electrons are added; both Sb_3^{3-} and ozone have isomers with equilateral structure.

It thus appears possible to create ozone-analogous systems by addition of three alkali electron donor atoms to an Sb_3 cluster nucleus. With increasing electron transfer from the alkali to the antimony subsystem, i.e., as one goes from A = Na to A = Rb, two trends are observed that liken A_3Sb_3 to both Sb_3^{3-} and ozone. First, the two C_{2v} minima around an Sb_3 opening angle of $\alpha = 60.0°$, which emerge from pseudo-Jahn−Teller distortion of the equilibrium geometry, grow together, corresponding to a weakening of the pseudo-Jahn−Teller effect. Second, an additional stable geometry of A_3Sb_3 with a large Sb_3 opening angle gains in stability over the two other equilibrium states identified for A_3Sb_3 and turns out to be the ground-state geometry of Rb_3Sb_3. The ionic species $Na_4Sb_3^+$ was shown to share all distinctive features with the isoelectronic unit Na_3Sb_3.

These observations are in accordance with the ZKB principle and its prediction of structural invariance of a system under isoelectronic substitution of its constituents with simultaneous addition of alkali electron donors.

The system ASb_3 in spin triplet configuration gives an example of the application of the ZKB principle in an extended sense that includes spin transfer. The spin transferred from the alkali metal atom to the Sb_3 unit stabilizes Sb_3 in D_{3h} symmetry and creates a C_{2v} ground state with a large opening angle, thus producing again an ozone-analogous structure.

The conclusions presented here for the various geometries predicted could in principle be tested indirectly through experimental observation of the associated rotational, vibrational, and electronic spectra as well as nuclear quadrupole interactions of the ^{121}Sb nuclei. The nuclear quadrupole interaction parameters have been shown elsewhere[27] to be very sensitive to the equilibrium geometries of alkali−antimony clusters. All these properties can be obtained quantitatively by standard procedures, requiring in the case of electronic transitions a knowledge of excited states and for vibrational spectra the energy derivatives with respect to the appropriate symmetrized coordinates. Although these calculations are time-consuming, they would be worthwhile to carry out when the respective experimental data become available.

As in our foregoing research on Sb_4-based cluster species,[4] the Zintl concept, although originally believed to apply to solid and liquid systems only, has been proven to be a heuristic idea of great value in the explanation and interpretation of numerous findings related to cluster geometries and stabilities.

Acknowledgment. The authors are grateful to Professor A. Welford Castleman, Jr. and Dr. A. Hartmann whose mass spectrometric measurements of alkali metal atom−antimony clusters have stimulated this work.

References and Notes

(1) Zintl, E. *Angew. Chem.***1939**, *1*, 52.
(2) Hoffmann, R. Solids and Surfaces; VCH Publishers: New York, 1988; Vol. 3.
(3) Schafer, H.; Eisenmann, B.; Muller, W. *Angew. Chem.* **1974**, *12*, 694.
(4) Hagelberg, F.; Srinivas, S.; Sahoo, N.; Das, T. P.; Weil, K. G. *Phys. Rev. A* **1996**, *53*, 353.
(5) Sattler, K.; Muhlbach, J.; Pfau, P.; Recknagel, E. *Phys. Lett*. **1982**, *87A*, 418.
(6) Zhang, H. X.; Balasubramanian, K. *J. Chem. Phys*. **1992**, *97*, 3437.
(7) Hagelberg, F.; Sahoo, N.; Das, T. P.; Weil, K. G.; Speidel, K. H. *Phys. Rev. A* **1992**, *46*, 6087.
(8) Hagelberg, F.; Neeser, S.; Sahoo, N.; Das, T. P.; Weil, K. G. *Phys. Rev. A* **1994**, *50*, 557.
(9) Scheuring, T.; Weil, K. G. *Surf. Sci*. **1985**, *156*, 457.
(10) Hartmann, A.; Castleman, A. W., Jr. In *Physics and Chemistry of Finite Systems: From Clusters to Crystals*; Kluwer Academic Publishers: Dordrecht, Boston, London, 1992; Vol. II, p 1121.
(11) Hartmann, A.; Weil, K. G. *Angew. Chem*. **1988**, *27*, 1091.
(12) Cotton, F. A.; Wilkinson, G. *Advanced Inorganic Chemistry*, 5th ed.; John Wiley & Sons: New York, 1988; p 453. Tanaka, T.; Morino, Y. *J. Mol. Spectrosc*. **1970**, *33*, 538.
(13) Stanton, J. F.; Lipscomb, W. N.; Magers, D. H.; Bartlett, R. J. *J. Chem. Phys*. **1989**, *90*, 1077. Stanton, J. F.; Bartlett, R. J.; Magers, D. H.; Lipscomb, W. N. *Chem. Phys. Lett*. **1989**, *163*, 333.
(14) Hay, P. J.; Wadt, W. R. *J. Chem. Phys.***1985**, *82*, 270.
(15) Wadt, W. R.; Hay, P. J. *J. Chem. Phys*. **1985**, *82*, 284.
(16) Hay, P. J.; Wadt, W. R. *J. Chem. Phys*. **1985**, *82*, 299.
(17) Huzinaga, S.; Andzelm, J.; Klobukowski, M.; Radzio-Andzelm, E.; Sakai, Y.; Tatewaki, H. *Gaussian Basis Sets for Molecular Calculations*; Elsevier: New York, 1984.
(18) Balasubramanian, K.; Sumathi, K.; Dai, D. *J. Chem. Phys*. **1991**, *95*, 3494.
(19) Cabaud, B.; Horeau, A.; Nounou, P.; Uzan, R. *Int. J. Mass Spectrom. Ion Phys*. **1973**, *11*, 157.
(20) Kordis, J.; Gingerich, K. A. *J. Chem. Phys.* **1972**, *58*, 5141.
(21) Frisch, M. J.; Trucks, G. W.; Head-Gordon, M.; Gill, P. M. W.; Wong, M. W.; Foresman, J. B.; Johnson, B. G.; Schlegel, H. B.; Robb, M. A.; Replogle, E. S.; Gomperts, R.; Andres, J. L.; Raghavachari, K.; Binkley, J. S.; Gonzalez, C.; Martin, R. L.; Fox, D. J.; Defrees, D. J.; Baker, J.; Stewart, J. J. P.; Pople, J. A. *Gaussian 92*, Revision A; Gaussian Inc.: Pittsburgh, PA, 1992.
(22) Mulliken, R. S. *J. Chem. Phys*. **1962**, *36*, 3428.

(23) Cotton, F. A. *Chemical Applications of Group Theory*, 2nd ed.; John Wiley & Sons: New York, 1990; p 125.
(24) Fantucci, P.; Koutecky, J.; Pacchioni, G. *J. Chem. Phys*. **1983**, *80*, 325.
(25) Renner, E. *Z. Phys*. **1934**, *92*, 172.
(26) See, for instance, the following. Alberty, R. A. *Physical Chemistry*, 6th ed.; John Wiley & Sons: New York, Chichester, Brisbane, Sydney, Toronto, Singapore, 1983.
(27) Hagelberg, F.; Das, T. P.; Weil, K. G. *Z. Naturforsch*., *A* **1996**, *51*, 557.